Polymer Journal (2014) 46, 584–591

www.nature.com/pj

ORIGINAL ARTICLE

# The structure and viscoelasticity of novolac resins

Satoshi Maji[1], Osamu Urakawa[2] and Tadashi Inoue[2]

**In this work, we discuss the dynamic viscoelasticity of three novolac resins with different molar masses and methylene linkage patterns (para–para′, ortho–ortho′ and ortho–para′ methylene linkages) to clarify the relationship between the structure and viscoelastic properties of novolac resins. The linkage patterns of the novolacs were evaluated using $^{13}C$ nuclear magnetic resonance spectroscopy. Gel permeation chromatography (GPC) measurements showed that the number density distribution was similar to that predicted for hyperbranched chains. The dependence of the intrinsic viscosity on the molar mass indicated that the three novolacs had a compact branched chain structure similar to that of hyperbranched chains. The glass transition temperatures determined by differential scanning calorimetry (DSC) depended on the molar mass and were less sensitive to the methylene linkage pattern. The viscoelastic spectra obtained by the time–temperature superposition principle for the three resins were similar to each other because the glassy relaxation properties were dominant. Weak polymeric modes originating from the chain connectivity were observed at low frequencies in the composite curve and were well described by the dynamic scaling theory for hyperbranched chains. A clear effect from the linkage patterns on the mechanical properties was not observed.**
*Polymer Journal* (2014) **46,** 584–591; doi:10.1038/pj.2014.27; published online 28 May 2014

**Keywords:** dynamic scaling; novolac; percolation; random branched chain

## INTRODUCTION

Phenolic resins are thermosetting resins that have attracted considerable attention as promising polymeric materials with excellent mechanical properties.[1] Phenolic resins are the oldest type of industrial plastic and were invented by Baekeland in 1907. Since then, these materials have been widely used as insoluble and infusible thermosetting resins in the electronics, automotive, housing and other industries. In particular, these polymers have been employed in automotive applications for the design of high fuel efficiency cars intended for use in a sustainable energy society in the near future, where light-weight and high-strength plastics are desired as a substitute for metals.

Polymerization involving monomers with a functionality greater than two, as in phenolic resins, has led to the formation of branched polymers and ultimately gels. The problem of polymer gelation has been recognized as a phase transition in connectivity, and percolation theory has been used to interpret both the static and dynamic data.[2–4] There are two universal classes for the gelation problem, and these are separated by the Ginzburg criterion that depends upon the chain length between branch points, $N$,[5,6] and the concentration of any nonreacting solvent.[7] In the absence of a solvent, the vulcanization of long linear polymer chains (large $N$) belongs to the mean field class and is modeled by the Flory–Stockmayer theory.[8–10] Critical percolation (small $N$) describes the polymerization of small multifunctional monomers.[2,11,12]

Novolacs are phenol–formaldehyde resins with a formaldehyde-to-phenol molar ratio of less than one and are prepolymers for cured phenolic resins. Polymerization is completed using acid catalysts such as oxalic, hydrochloric or sulfonic acids. Novolacs dissolve in organic solvents. A representative chemical structure for a novolac is shown in Figure 1. Methylene groups act as linkages between two phenol units. The methylene linkage groups can be classified into three types, ortho–ortho′ ($o$–$o'$), ortho–para′ ($o$–$p'$) and para–para′ ($p$–$p'$), according to the three positions that are adjacent to the hydroxyl group of the phenolic ring. Because novolacs are the prepolymers of phenolic resins, the same linkage patterns are observed in phenolic resins themselves. It is expected that the physical properties of novolacs and phenol resins depend on the methylene linkage patterns. However, this difference has not yet been determined in detail because the structural analysis of phenolic resins is difficult because of their insolubility and infusibility. In this study, the relationship between the chain structure and rheological properties of well-characterized novolacs is investigated. The effect of linkage patterns on the viscoelastic properties is introduced. To accomplish these tasks, we conducted nuclear magnetic resonance (NMR) spectroscopy, gel permeation chromatography (GPC), differential scanning calorimetry (DSC) and rheological measurements, including dynamic birefringence. The results show that the viscoelastic data can be explained by the structural data.

The viscoelasticity of randomly branched polymers can be analyzed using the dynamic scaling theory based on the Rouse model.[4,13,14] The theory is applicable to enough long chains at reaction degrees near the gel point. However, for short chains just after the reaction starts, the glassy nature of the material contributes significantly to the

[1]S.B. RESEARCH CO., LTD, Utsunomiya, Japan and [2]Department of Macromolecular Science, Graduate School of Science, Osaka University, Toyonaka, Japan
Correspondence: Professor T Inoue, Department of Macromolecular Science, Graduate School of Science, Osaka University, 1-1 Machikaneyama, Toyonaka 560-0043, Japan.
E-mail: tadashi@chem.sci.osaka-u.ac.jp
Received 10 January 2014; revised 17 March 2014; accepted 18 March 2014; published online 28 May 2014

viscoelastic spectra, making the interpretation of viscoelastic properties rather complicated. In this study, the viscoelastic properties of novolacs were analyzed by considering the glassy nature and randomly branched chain structure. First, the structures of the novolacs with different molar mass distributions and methylene linkage patterns were determined. The dynamic moduli of the three novolac resins were then measured, and the viscoelastic spectra were reproduced using the dynamic scaling theory and including the glass contribution. The results show that the viscoelastic properties of novolacs are well described through a combination of polymeric and glassy modes. Rheo-optical characterization using birefringence measurements enabled the quantitative separation of the modulus into polymeric and glassy modes.[15] However, the measurements on oligopolymers were not as straightforward. This is because measurements of the shear deformations are necessary that requires a large correction for apparatus compliance. Finally, we demonstrate that the rheo-optical data can be consistently described as the sum of the polymeric and glassy modes, although it should be noted that the frequency range of the data is limited because of the large compliance correction.

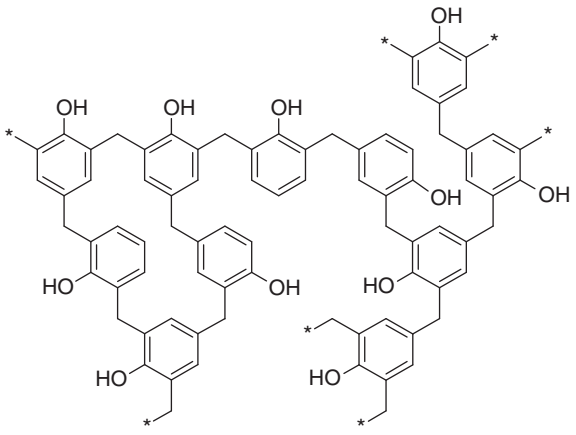


**Figure 1** Molecular structure of the novolacs. Adjacent phenolic groups are connected by methylene linkers.

## EXPERIMENTAL PROCEDURE

Typical phenolic resins, that is, random novolac and high ortho novolac, were supplied by Sumitomo Bakelite Co., Ltd (Tokyo, Japan). The molar masses and molar mass distributions of the novolac samples were determined by GPC (Tosoh, Tokyo, Japan) and right-angle light scattering/Visco detector (TDA302; Viscotek, Houston, TX, USA). The bulk density, $d$, of the novolacs was estimated to be 1.23 g cm$^{-3}$. The structures of the novolac resins in a methanol solution were characterized by $^{13}$C NMR spectroscopy (ECA-400; JEOL, Tokyo, Japan). The glass transition temperature was measured using a modulated differential scanning calorimeter (MDSC 9200; TA Instruments, New Castle, DE, USA). In the modulated DSC experiments, the heating and cooling rates were 2 K min$^{-1}$ and the modulation rate was $\pm$2 K min$^{-1}$. During the first run, the temperature was increased from 223 to 473 K and then decreased to 223 K. During the second run, the temperature was increased to 473 K once again. The glass transition temperature was determined by reversing the heat flow during the second run.

The complex shear moduli, $G^*$, of the novolac samples were measured on an ARES rheometer (TA Instruments) with a standard parallel plate fixture with a diameter of 8 mm and a home-made parallel plate fixture with a diameter of 4 mm. Instrument compliance was carefully corrected using the method reported by McKenna and coworkers[16,17] The composite curves were generated for the complex moduli measured over a temperature range from 320 to 430 K, following the method of reduced variables.[18]

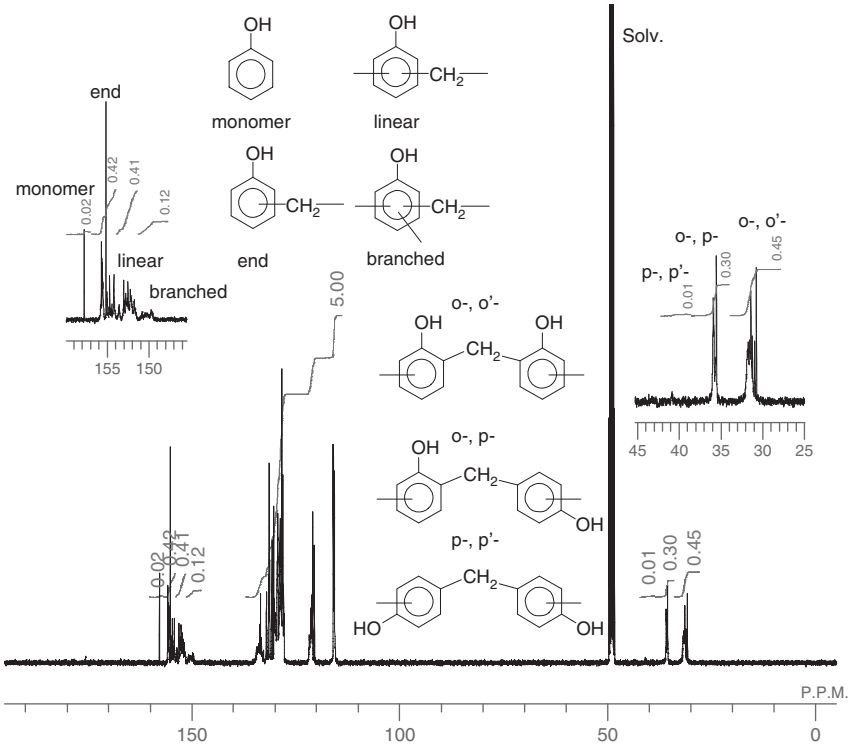


**Figure 2** The $^{13}$C nuclear magnetic resonance (NMR) spectrum of ON1800. The full colour version of this figure is available at *Polymer Journal* online.

## RESULTS AND DISCUSSION

### $^{13}$C NMR spectroscopy

An example of a $^{13}$C NMR spectrum of a novolac resin is shown in Figure 2. The signals from the carbon atoms of the benzene ring are observed at ~158 p.p.m., and the methylene carbons give rise to signals at ~30–37 p.p.m. The intensities of the signals for the benzene ring carbon allow the following fractions to be determined: (1) monomer, (2) end (mono-substituted), (3) linear (bi-substituted) and (4) branched (tri-substituted) (see Figure 2). The results are summarized in Table 1. The ON1800 has a higher fraction of end-type phenyl groups than the ON7800. The number of branched benzene rings is approximately one-third of the number of linear units. The fraction of branched units is almost the same for each of the three novolacs. From these values it is estimated that the branching occurs on average for every four repeated units.

By assuming that no cyclic structures were present, the number average molar mass, $M_n$, can be calculated from:

$$M_n^{\mathrm{NMR}} = \frac{d}{N_{\mathrm{chain}}} = \frac{2d}{N_{\mathrm{end}} - N_{\mathrm{branch}}} \quad (1)$$

where $d$ is the density, $N_{\mathrm{chain}}$ is the molar density of the chain and $N_i$ ($i$ = monomer, end, linear and branched, as shown in Figure 2) is the molar density of the $i$-th type of phenol unit. Because one branching point increases the number of chain ends by one, $(N_{\mathrm{end}} - N_{\mathrm{branch}})/2$ corresponds to $N_{\mathrm{chain}}$. The variable $N_i$ can be related to the number fraction of $i$, defined as $n_i$, and determined by the NMR measurements:

$$N_i = \frac{d}{M_0} n_i \quad (2)$$

where $M_0$ is the molar mass of the repeating unit. The obtained $M_n^{\mathrm{NMR}}$ values are listed in Table 2. In the case of ON1800, $M_n^{\mathrm{NMR}}$ is consistent with the number of average molar mass determined by the GPC, $M_n^{\mathrm{GPC}}$. The agreement between $M_n^{\mathrm{NMR}}$ and $M_n^{\mathrm{GPC}}$ is quite good with the exception of ON7800. The reason for this discrepancy is not clear. The presence of cyclic structures decreases the number of chain ends. Therefore, $M_n^{\mathrm{NMR}}$ may yield a larger value. Consequently, the existence of cyclic structures does not explain the lower $M_n^{\mathrm{NMR}}$ value obtained for ON7800.

The number of branching points per chain, $\nu_B$, can be determined from:

$$\nu_B = \frac{N_{\mathrm{branch}}}{N_{\mathrm{chain}}} \quad (3)$$

where $\nu_B = 0$ corresponds to the linear chains. For all of the novolacs studied, $\nu_B$ is ~1.5 (see Table 2). This indicates that the novolacs on average include approximately one or two branching points per chain. It is worth noting that $\nu_B$ increases with the molar mass of the chain. A lower $\nu_B$ reflects a smaller chain size of novolacs. As previously discussed and shown in Table 1, the ratio of $n_{\mathrm{linear}}/n_{\mathrm{branch}}$ is ~3, indicating that branching occurs at every four phenolic units.

The extent of the linkage reaction, $p$, can be evaluated from the value of $n_i$:

$$p = \frac{n_{\mathrm{end}} + 2n_{\mathrm{linear}} + 3n_{\mathrm{branch}}}{3} \quad (4)$$

The $P$-values obtained are summarized in Table 2.

The contents of the methylene linkage patterns, such as the $p$–$p'$ linkages, were calculated from the chemical shifts of methylene group signals. The results are summarized in Table 3. RN7200 has an approximately equal number of *para* and *ortho* linkages. If we assume that the reactivity of each *ortho* or *para* position of the benzene ring is independent of substitutions at other sites and further assume that the reactivity of the *ortho* site is $r$ times higher than at the *para* site, then the distribution ratio of various methylene linkage types can be obtained as $4\{r/(2r+1)\}^2$ for $o$–$o'$ methylene linkages, $4r/(2r+1)$ for $o$–$p'$ linkages and $\{1/(2r+1)\}^2$ for $p$–$p'$ linkages. This analysis indicates that the reactivity of the *ortho* site is 1.64 times higher than at the *para* site for ON1800 and ON7800, whereas the *ortho* site is half as reactive as the *para* site in RN7200.

Using the $r$ and $P$-values, we can calculate the $n_i$ values. These results are compared with the experimental data in Table 1, showing good agreement and indicating that the methylene linkage reaction occurred statistically. The critical extent of the reaction, $p_C$, assuming that $M = \infty$, was estimated to be 0.87–0.89 if we assume a fixed $r$ value, irrespective of the $P$-value. At $P = p_C$, the mole fraction of the branched benzene rings is ~60%, and the rest of the polymer is formed by linear benzene rings. This calculation indicates that the average monomer number between the crosslinking points is ~1. Note that the present system is far from the gel point because the $P$-value for the samples being discussed is ~0.54.

### GPC and intrinsic viscosity

*Molar mass distribution.* The dependence of the molar mass, $M$, on the weight fraction, $W_x$, obtained by the GPC measurements is shown in Figure 3. The oscillations of $W_x$ in the low $M$ region are because of the discrete dependence of $M$ on the oligomers. The variable $M$ was

**Table 1 Characterization of chain end and branching units in novolacs**

| | Experimental | | | | Calculated | | | |
|---|---|---|---|---|---|---|---|---|
| Sample code | Monomer | End | Linear | Branch | Monomer | End | Linear | Branch |
| ON1800 | 0.0170 | 0.442 | 0.418 | 0.122 | 0.0892 | 0.347 | 0.418 | 0.146 |
| ON7800 | 0.0953 | 0.333 | 0.419 | 0.154 | 0.0884 | 0.345 | 0.419 | 0.147 |
| RN7200 | 0.0481 | 0.385 | 0.412 | 0.155 | 0.0800 | 0.376 | 0.412 | 0.131 |

**Table 2 Molar mass, degree of branching and extent of reaction of novolacs**

| Sample code | $M_n^{NMR}$ g mol$^{-1}$ | $M_n^{GPC}$ g mol$^{-1}$ | $M_w^{GPC}$ g mol$^{-1}$ | $\nu_B$ | P | $p_C$ |
|---|---|---|---|---|---|---|
| ON1800 | 663 | 658 | 1800 | 0.7 | 0.546 | 0.8687 |
| ON7800 | 1140 | 1660 | 16 100 | 1.5 | 0.541 | 0.8712 |
| RN7200 | 922 | 947 | 4410 | 1.2 | 0.559 | 0.8902 |

Abbreviations: GPC, gel permeation chromatography; NMR, nuclear magnetic resonance.

**Table 3 Characterization of methylene linkage types of novolacs**

| | Experiment | | Calculated | | | | | |
|---|---|---|---|---|---|---|---|---|
| Sample code | o-, o'- | o-, p'- | p-, p- | o-, o- | o-, p- | p-, p- | Reactivity ratio of o/p | Remarks |
| ON1800 | 0.59 | 0.39 | 0.01 | 0.59 | 0.36 | 0.05 | 1.65 | High ortho |
| ON7800 | 0.59 | 0.41 | 0.00 | 0.59 | 0.36 | 0.05 | 1.63 | High ortho |
| RN7200 | 0.27 | 0.49 | 0.24 | 0.25 | 0.50 | 0.25 | 0.50 | Random |

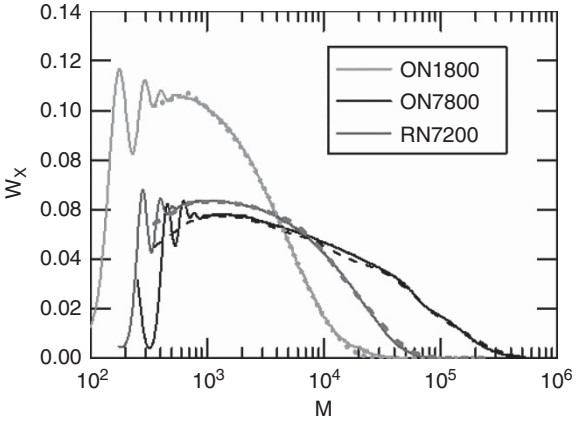


**Figure 3** Molar mass dependence of the weight fraction obtained by gel permeation chromatography (GPC) measurements. The dotted lines represent the fitting results using Equation (5). The full colour version of this figure is available at *Polymer Journal* online.

determined using the light scattering apparatus. ON1800 was found to have the lowest molar mass, and ON7800 was found to have a markedly broader molar mass distribution. The $M_w$ and $M_n$ values are summarized in Table 2. The $M_n$ values are consistent with those obtained by NMR spectroscopy.

The number densities of the polymers with mass $M$, $n(M)$, were calculated from Figure 3, and the results are shown in Figure 4. A power law for $n(M)$ holds in the intermediate mass region for all the samples, and $n(M)$ deviates from this power law over a certain molar mass. These features are captured by the percolation theory, and $n(M)$ was fitted to a power law times a shifted Gaussian cutoff function[19,20] of the form:

$$n(M) = A\left(\frac{M}{M_{\mathrm{chat}}}\right)^{-\tau} F\left(\frac{M}{M_{\mathrm{chat}}}\right) = A\left(\frac{M}{M_{\mathrm{chat}}}\right)^{-\tau} \exp\left[\left\{Z_{\max} - \left(\frac{M}{M_{\mathrm{chat}}}\right)^{\sigma}\right\}^2\right], \quad (5)$$

where $A$ is a numerical constant and $F(x)$ is a cutoff function. The power law represents the fractal nature of chain structure, and the cutoff function is related to the maximum size of the chain. Numerical simulations showed a maximum $F$ was achieved for a nonzero value of the reduced parameter, $Z_{\max}$, and the numerical data were well described by the aforementioned Gaussian curve.[19] The results of fitting the data to Equation 5 are shown in Figure 4. Theoretical agreement is satisfactory with the exception of the oligomer region. The exponents $\tau$ and $\sigma$ are summarized in Table 4 and are determined to be 2.2 and 0.46, respectively, using the critical percolation theory, and 5/2 and 1/2 using the Flory–Stockmayer approach.[2,13] The experimental results are inconsistent with these values and are rather similar to $\tau = 1.5$ for hyperbranched polymers. Here, hyperbranched polymers indicate that the polymers synthesized from a monomer ($AB_{f-1}$) that has one functional group (type A) that differs from the $f-1$ other groups (type B) such that only group A can react with group B. However, reactions between two A or two B groups are impossible. This incisive constraint indicates that the reaction is no longer random. The structure of a hyperbranched polymer from $AB_{f-1}$ is the same as that for the randomly branched polymers from $A_f$ with an $f$ reaction site, but the molar mass distribution is different.[4] Because the experimental results show that $\tau$ is $\sim 1$ and $\sigma$ is $\sim 0.4$, the novolacs are fairly similar in nature to

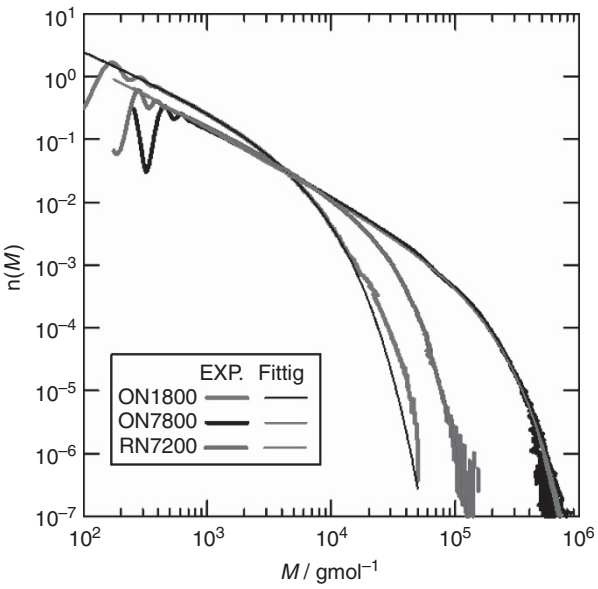


**Figure 4** Gel permeation chromatography (GPC) data for the novolacs. The curves are two-parameter nonlinear fits to Equation (5) using the percolation values for the exponents $\tau$ and $\sigma$. The full colour version of this figure is available at *Polymer Journal* online.

**Table 4 Static exponents for molar mass distribution**

| *Sample* | $\tau$ | $\sigma$ | $M_{char}$ | $\theta$ |
|---|---|---|---|---|
| ON1800 | 0.987 | 0.34 | 1252 | 1.0 |
| ON7800 | 1.2 | 0.4 | 40600 | 1.1 |
| RN7200 | 1.11 | 0.46 | 7900 | 1.0 |

hyperbranched polymers. The agreement with hyperbranched polymers can be consistently attributed to the fact that the reactivity of the *ortho* and *para* sites is not the same. Another reason is that the extent of the linkage reaction, $p$, is far from the percolation threshold, $p_c$. For systems that are far from the percolation threshold or hyperbranched systems in $AB_2$-type monomers, the number density distribution can be described as:[2,4]

$$n(M) = B\left(\frac{M}{M_{\mathrm{char}}}\right)^{-\theta} g\left(\frac{M}{M_{\mathrm{char}}}\right) = B\left(\frac{M}{M_{\mathrm{char}}}\right)^{-\theta} C^{\left(\frac{M}{M_{\mathrm{char}}}\right)}, \quad (6)$$

where $B$ and $C$ are constants. This scaling is believed to be valid irrespective of the extent of the reaction if the system is far from the critical point.[2] The exponent $\theta$ is determined to be 1 for two-dimensional systems and $\theta = 1.5$ for three-dimensional systems.[2,4] Deviation from $\theta = 1.5$ might be related to the difference in the reactivity of the *ortho* and *para* sites.

It is important to note that the average molar mass of the three novolacs is not particularly high, but the molar mass distribution is quite wide in the case of ON7800. In addition, the characteristic molar mass in the cutoff function $M^* \sim M_Z$ for ON7800 was found to be $> 10^5$.

*Chain dimension.* The relationship between the intrinsic viscosity, $[\eta]$, and the molar mass obtained by the GPC right-angle light scattering/Visco detector is shown in Figure 5. These data also include the relationship for bisphenol A polycarbonate in tetrahydrofulan (THF).[21] The $[\eta]$ values of the novolacs are very similar to each other

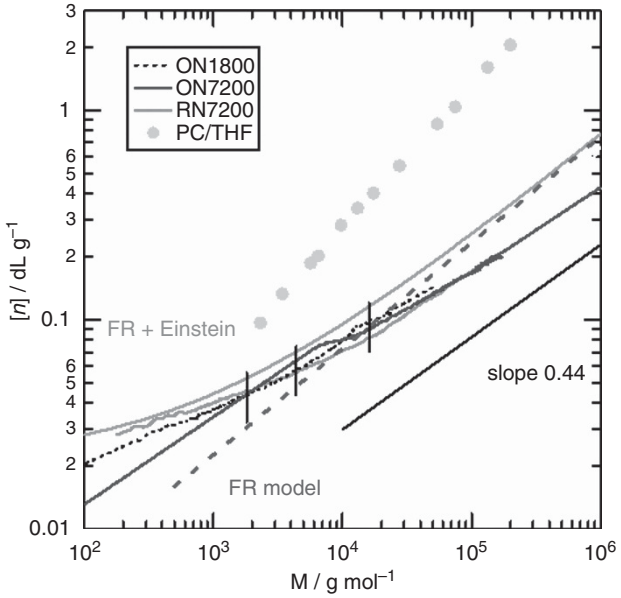


**Figure 5** Molar mass dependence of the intrinsic viscosity for the novolacs in tetrahydrofulan (THF). The green circles represent the intrinsic viscosity of the bisphenol A polycarbonate in THF. The full colour version of this figure is available at *Polymer Journal* online.

and are lower than those for the other polymers, indicating that the effect of the methylene linkage pattern is small. Because [η] corresponds to the specific volume of the chain, the lower [η] values of the novolacs indicate a smaller and more compact chain structure than for the polycarbonate.

The intrinsic viscosity can be estimated from the chain dimension. The purple dotted line in Figure 5 represents the theoretical value based on a freely rotating chain for linear chains:[22]

$$[\eta] = \Phi \frac{\langle R^2 \rangle^{\frac{3}{2}}}{M} \tag{7}$$

$$\langle R^2 \rangle = N b_{\text{eff}}^2. \tag{8}$$

Here, $\Phi$ is the Flory viscosity coefficient ($\Phi = 2.87 \times 10^{23}$), $N$ is the number of bonds per chain and $b_{\text{eff}}$ is the effective bond length. The $b_{\text{eff}}$ of the freely rotating chains is related to the bond length, $b$, and the bond angle, $\theta_i$, at the $i$-th unit. The novolacs have two bond angles at the methylene units and benzene rings. Therefore, $b_{\text{eff}}$ is related to $b$ through the following equation:

$$b_{\text{eff}}^2 = \frac{1}{2}\left(\frac{1-\cos\theta_1}{1+\cos\theta_1} + \frac{1-\cos\theta_2}{1+\cos\theta_2}\right) b^2. \tag{9}$$

The value of $b_{\text{eff}}$ is estimated to be 0.74 nm with $b = 0.294$ nm, $\theta_1 = 120^\circ$ and $\theta_2 = 109.5^\circ$. The calculated [η] is shown in Figure 5. The experimental value of [η] is higher than the calculated value in the low $M$ region ($M$/g mol$^{-1}$ $< 10^4$) and is lower in the high $M$ region.

In this calculation, the chain is regarded as a thin strand and, therefore, the intrinsic volume of chain is ignored. For short chains, the inclusion of the volume of the repeating units is required. The addition of the Einstein sphere viscosity, $[\eta]_E$, provides better agreement in the low $M$ region:

$$[\eta] = \Phi \frac{\langle R^2 \rangle^{\frac{3}{2}}}{M} + [\eta]_E, \tag{10}$$

$$[\eta]_E = \frac{2.5}{d}, \tag{11}$$

where $d$ is the density. The result derived from Equation (9) shows the best agreement in the low mass region (Figure 5). The [η] values of the novolacs are lower than those of the freely rotating chain in the high $M$ region, indicating that the novolacs have a compact chain dimension because of branching.

In the high $M$ region, [η] behaves similarly to a power law, $[\eta] \propto M^a$.[13] The exponent $a = 0.44$ is very similar to that for a swollen fractal dimension of the randomly branched polymer $a = 0.45$,[23] suggesting that the chain dimension of the novolacs is similar to that of a randomly branched chain. Note that the chain dimension for hyperbranched chains agrees well with randomly branched chains.[4] According to Equation (10), the exponent $a = 0.44$ provides $\langle R^2 \rangle \propto M^{0.96}$ and, therefore, the fractal dimension $D$ is 2.08 ($= 2/0.96$). This value is inconsistent with the value of 2.53 for the fractal dimension of the randomly branched chain. This inconsistency arises because Equation (10) works satisfactorily for flexible linear chains, but in the case of branched chains, the Φ coefficient depends on the hydrodynamic interactions between the segments[22] and can be expected to slightly increase with the branching density. The change in the $\Phi$ parameter can be considered assuming power law behavior, $\Phi \sim \Phi\ M^{0.29}$,[23] yielding $D = 3/(a + 1 - 0.29) \sim 2.6$.

In conclusion, the molar mass distribution did not follow the scaling rule derived from the percolation theory for randomly branched chains. This indicates that the present system does not follow statistically random branching and is similar to the hyperbranched chains originating from the $AB_{f-1}$ monomers because of the difference in the reactivity of the three sites in the monomer. The molar mass dependence of [η] also strongly suggests that the chain dimensions of the novolacs are similar to those of hyperbranched polymers.

**Modulated DSC**

The results of modulated DSC are provided in Supplementary Information. Increases in the heat capacities because of the glass transition were observed at ~336 K by reversing the heat flow for each sample. The glass transition temperature observed during the second run is ~20 K higher than during the first run. This change is attributed to the reduction in the level of residual monomer and the relaxation enthalpy of the novolacs. When using modulated DSC, the total heat flow is represented by a summation of the reversible and nonreversible heat flows:

$$\frac{dH}{dt} = C_P \frac{dT}{dt} + f(T,t). \tag{12}$$

The first term on the right-hand side of the equation represents the reversible heat flow that is associated with heat capacity, melting and the glass transition. The second term on the right-hand side of the equation corresponds to the nonreversible heat flow that is associated with chemical reactions, crystallization, evaporation, resolution and enthalpy relaxation. The results from the first run for the nonreversible heat flow of the novolacs show an enthalpy relaxation occurring at ~310 K and an endothermic polymerization reaction from the residual monomer occurring at ~340 K. During the second run for nonreversible heat flow of the novolacs, evidence for enthalpy

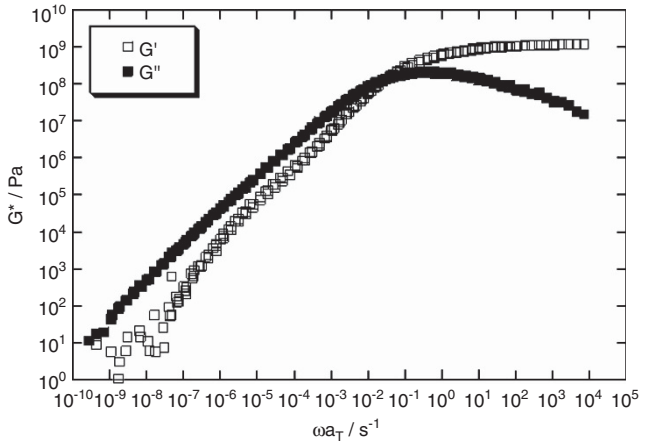


**Figure 6** Complex shear viscoelasticity of ON7800 (the reference temperature is 353 K).

relaxation and endothermic reaction was not observed, indicating that the novolac resins relax upon being heated to 473 K.

### Complex shear modulus

*Overview.* The composite curves for the complex shear moduli, $G^*$, for the novolac resins are shown in Figure 6. The method of reduced variables was used to obtain these curves.[18] In each of the $G^*$ curves, a relaxation mode is observed for $G'$ as a shoulder in the $10^5$ Pa range (in addition to the glassy relaxation in the $10^8$ Pa range). These relaxation modes can be assigned to different polymeric modes (the Rouse mode) because the molar masses of these samples are in the range 1000–10 000. Similar $G^*$ curves have been reported for low-molecular-weight polystyrenes.[24]

*Temperature dependence.* All of the samples have similar viscoelastic spectra and shift factors, $a_T$. The shift factors for all the samples are shown in Figure 7. From comparing ON1800 and ON7800, it can be concluded that the shift factors for the novolac resins appear to be independent of molar mass, distribution and linkage patterns. The agreement between ON7800 and RN7200 suggests that the shift factor is independent of the type of linkage pattern. The continuous curve included in Figure 7 was calculated using the universal Williams–Landel–Ferry (WLF) equation:

$$\log a_T = \frac{c_1(T - T_r)}{c_2 + T - T_r} \tag{13}$$

where $c_1$ and $c_2$ are the WLF parameters. If $T_r = T_g + 50$ is chosen, the $a_T$ of a wide range of polymers yields a solution to the universal WLF equation for $c_1 = 8.86$ K and $c_2 = 101.6$ K. Compared with the WLF equation for the shift factor, the temperature dependence of $a_T$ for ON7800 and RN7200 is stronger than that for the universal WLF equation. The variable $T_g^{visco}$ is defined as the temperature at which the loss modulus shows a maximum at $\omega\,s^{-1} = 0.01$. The obtained $T_g^{visco}$ values are summarized together with $T_g$ values determined by DSC in Table 5.

*Comparison of frequency dependence.* The normalized viscoelastic spectra of the three novolac resins are shown in Figure 8. A horizontal shift was employed so that each tan δ versus ω is consistent with the others in the glassy zone. A very small vertical shift was also used for better superposition. It can be observed from Figure 8 that the ON7800 has the longest relaxation mode of the three novolacs

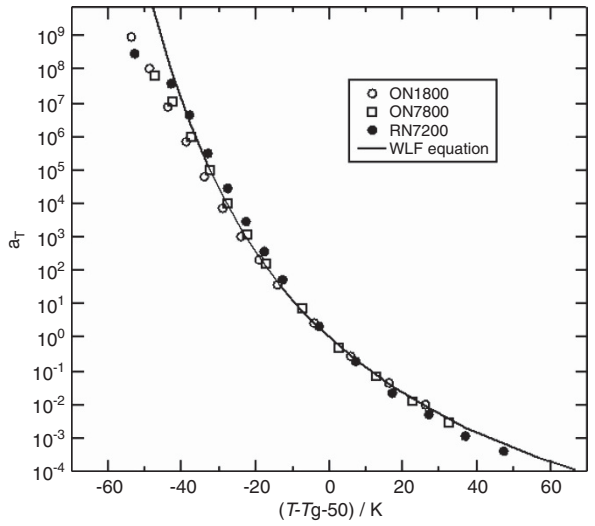


**Figure 7** Shift factors, $a_T$, for the novolac resins.

**Table 5 Glass transition temperatures of the novolacs**

| *Sample code* | $T_g^{DSC}$/K | $T_g^{visco}$/K |
|---|---|---|
| ON1800 | 327.1 | 324 |
| ON7800 | 340.5 | 344 |
| RN7200 | 335.9 | 344 |

Abbreviation: DSC, differential scanning calorimetry.
$T_g^{visco}$ is defined as the temperature at which the loss modulus shows a maximum at $\omega\,s^{-1} = 0.01$.

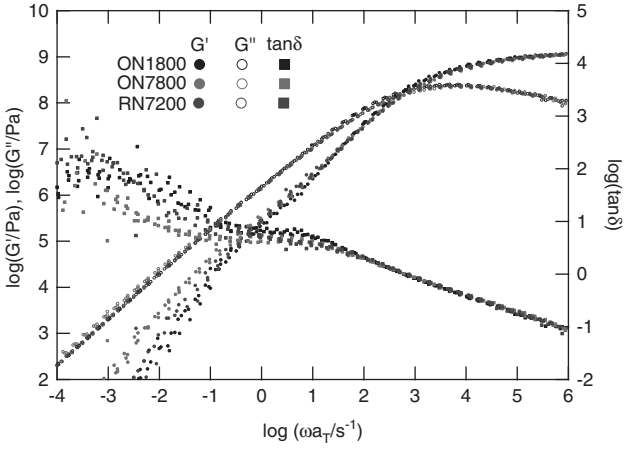


**Figure 8** Comparison of $G^*$ for the novolac resins. The full colour version of this figure is available at *Polymer Journal* online.

studied. This finding is consistent with ON7800 having the largest chain size.

Figure 9 shows a comparison of $G^*$ for ON7800 and the typical glassy response of amorphous polymers. In this case, the $G^*$ data for polystyrene, A1000 with $M_w = 1010$, were used.[24] The molar mass of the viscoelastic segment size for polystyrene is $\sim 1000\,g\,mol^{-1}$. Therefore, a polymeric mode is not observed for a $G^*$ of A1000. For $\log(\omega a_T\,s^{-1}) > 2$, the tan δ values of the two polymers are consistent with each other. At lower frequencies, the value of tan δ for

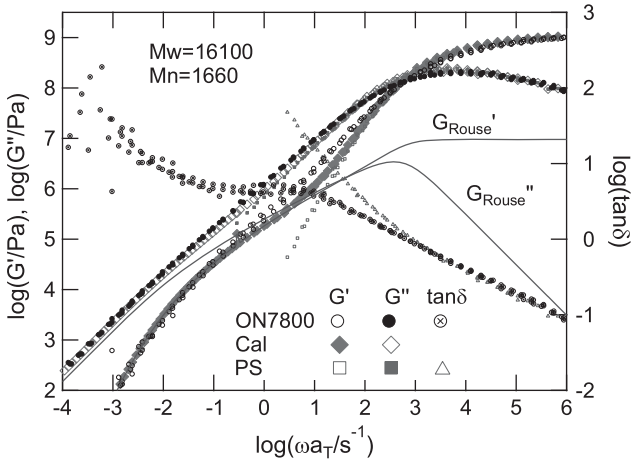


**Figure 9** Comparison of $G^*$ for ON7800 and the glassy modulus (polystyrene, $M_w = 1000$). The full colour version of this figure is available at *Polymer Journal* online.

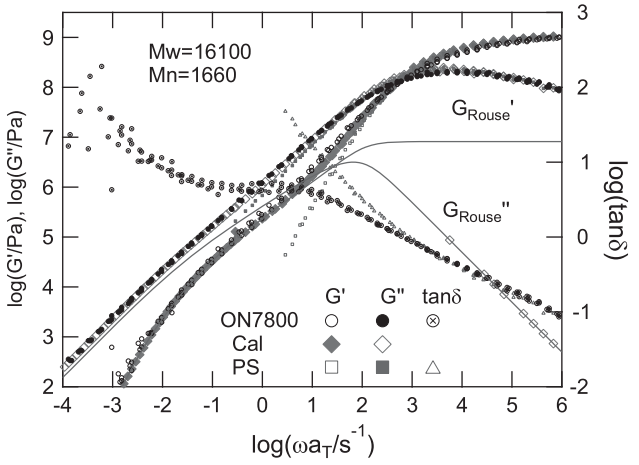


**Figure 10** Comparison of $G^*$ values from the experimental data and theoretical calculations for $\nu = 1/2.53$. The full colour version of this figure is available at *Polymer Journal* online.

A1000 increases quickly as ω decreases, indicating that A1000 has a narrower relaxation time distribution.

The viscoelastic properties for branched chains were studied using dynamic scaling based on the Rouse model. For a polymer chain composed of segments with $N$ beads of length $b$, the Rouse time $\tau_R$ is represented by the following equation:[25]

$$\tau_{\text{Rouse}} \approx \frac{\zeta b^3}{k_B T} N^{1+2\nu} \approx \tau_0 N^{1+2\nu}, \tag{14}$$

where $\zeta$ and $k_B$ are the friction coefficient of the beads and the Boltzmann constant, respectively. The parameter $\tau_0$ is the shortest Rouse relaxation time and $\nu$ is the fractal dimension of the chain. For an ideal linear chain, the exponent $\nu$ is 1/2. The polymeric modes (Rouse modes) of the branched chain, $G^*_{\text{Rouse}}$, can then be calculated from dynamic scaling.

As described, significant contributions from the glassy mode are observed in the viscoelastic spectra of the novolacs. Therefore, to provide a more detailed discussion, $G^*$ values for the novolacs were calculated using the following equations that consider the glassy modes:

$$G*(\omega) = G*_{\text{Rouse}}(\omega) + G*_{\text{A1000}}(\omega), \tag{15}$$

$$G^*_{\text{Rouse}} = \sum_i w(M_i) \frac{\rho RT}{M_i} G^*_i(\omega), \tag{16}$$

$$G^*_i(\omega) = \sum_{p=1}^{N_i} \frac{\omega^2 \tau_{i,p}^2 + i\omega\tau_{i,p}}{1 + \omega^2 \tau_{i,p}^2}, \tag{17}$$

$$\tau_{i,p} = \tau_0 \left(\frac{N_i}{p}\right)^{(1/\nu+2)/3}. \tag{18}$$

In the calculation of $G^*_{\text{Rouse}}(\omega)$, we first considered ordinary linear novolac chains, $\tau_{i,p} = \tau_0 (N_i/p)^2$, to assess the effect of branching. The Rouse segment size, $M_S$, was assumed to be $300\,\text{g mol}^{-1}$, and the results are shown in Figure 9. The value of $\tau_{\text{Rouse}}$ was chosen so that the calculated $G^*$ agreed with the experimental data at low frequencies. Consequently, agreement is good at these frequencies. However, for the middle frequency region, $-1 < \log(\omega a_T\,\text{s}^{-1}) < 2$, the $G'$ agreement clearly decreases. It should be noted that the shortest Rouse relaxation time, $\tau_S$, is very similar to the relaxation time of the glassy component $\tau_G$. For the ordinary polymers, a previous study showed that $\tau_S/\tau_G$ is $\sim 10$.[26] Thus, it can be concluded that the $G^*_{\text{Rouse}}$ of the novolacs should have a narrower relaxation time distribution because of the branching. This is quite natural because branching of the chain leads to the degeneracy of the longest relaxation mode.

As discussed, the molar mass dependence on $[\eta]$ suggests that the novolacs have a similar branching structure to hyperbranched chains. Because the structure of hyperbranched chains is identical to that of randomly branched chains, $G^*_{\text{Rouse}}$ was recalculated so that $\nu = 1/2.53$ for the randomly branched chain. The result is shown in Figure 10, and it demonstrates reasonably good agreement over the entire frequency region. Therefore, the viscoelastic analysis indicates that the novolacs can be regarded as consisting of randomly branched chains. This situation is consistent with the conclusion drawn from the NMR and intrinsic viscosity experiments.

*Rheo-optical data.* To more clearly observe the Rouse dynamics of the novolacs, it is useful to perform dynamic birefringence measurements.[15] The merit of the rheo-optical method is in the quantitative separation of the modulus into the component functions depending on the molecular origin of the stress with the modified stress optical rule.[15] This method has been previously applied to various systems.[27–30] For amorphous polymers, the complex modulus and complex strain-optical coefficient, $K^*(\omega)$, can be separated into the glassy, $G^*_G$, and the polymeric (rubber), $G^*_R(\omega)$, components:

$$G*(\omega) = G*_R(\omega) + G*_G(\omega), \tag{19}$$

$$K*(\omega) = C_R G*_R(\omega) + C_G G*_G(\omega), \tag{20}$$

where $C_R$ and $C_G$ are the stress-optical coefficient for the R and G components, respectively. If Equations (19) and (20) are treated simultaneously, we can determine $G^*_R$ and $G^*_G$. The separation is essentially identical to Equation (15). However, the applicability of the actual measurements from shear deformation is limited at values near the glass transition because of the necessary large apparatus compliance correction. The preliminary $G^*_R$ and $G^*_G$ results for RN7200 are shown in Figure 11. As predicted, the glassy component, $G^*_G$, agrees well with the $G^*$ value for low mass polystyrene and A1000, indicating that the glassy component of the novolacs is identical to the typical glassy component of amorphous polymers. However, the

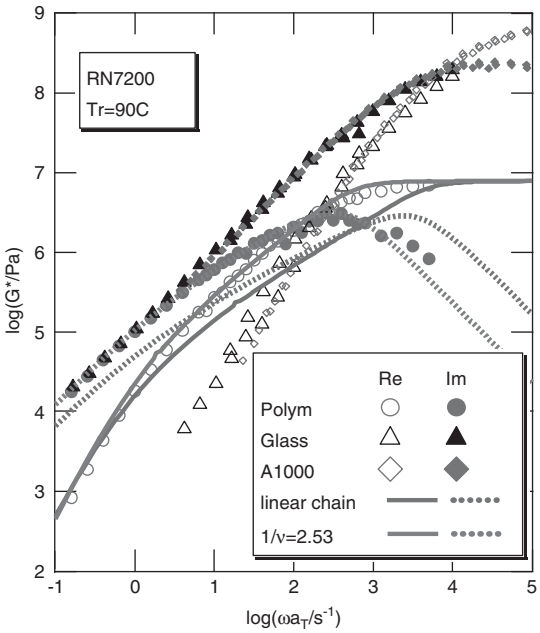


**Figure 11** Component functions for RN7200. The curves represent the complex moduli calculated using the Rouse model. The full colour version of this figure is available at *Polymer Journal* online.

polymeric component, $G^*_R$, is fitted to the Rouse model. In this case, $M_S = 350$ was used. The curves in the figure show the results for $(2+1/\nu)/3 = 1.5$ and 2. Once again, $(2+1/\nu)/3 = 1.5$ yields a better result that supports the conclusion outlined in the previous section.

## CONCLUSION

In this work, NMR, GPC, DSC and rheological measurements were carried out on three samples to determine the relationship between the structure and rheological properties of novolacs. The molar mass dependence on the number density did not follow the percolation theory for the randomly branched chains and was similar to that for a hyperbranched chain structure. The molar mass dependence on the intrinsic viscosity indicated that the novolacs had a hyperbranched chain structure. This result was obtained because the extent of reaction for the system is far from the percolation threshold and was also because of the different reactivities of the three sites in the benzene ring. The dynamic moduli of the three novolacs were similar, particularly in the glassy zone. A difference in the molar mass was observed at low frequencies. The dynamic modulus because of chain connectivity (polymeric modes) was estimated by subtracting the glassy modulus from the shear modulus that was well described by the dynamic scaling theory based on the Rouse model. The exponent for the polymeric modes was found to be $\sim 2/3$, consistent with dynamic scaling for randomly branched chains (the same as for hyperbranched polymers). The methylene linkage patterns *o*–*o*′, *o*–*p*′ and *p*–*p*′ in the phenolic rings did not significantly affect the scaling of the chain dimension and dynamic modulus.

## ACKNOWLEDGEMENTS

This study was partly supported by Grant-in-Aid for Scientific Research (No. 24350120) from the Japan Society for the Promotion of Science.

1 Gardziella, A., Pilato, L. A. & Knop, A. *Phenolic Resins: Chemistry, Applications, Standardization, Safety and Ecology* (Springer, Berlin, 1999).
2 Stauffer, D. & Aharony, A. *Introduction to Percolation Theory* (Taylor and Francis, London, 1992).
3 de Gennes, P. G. La percolation: Un concept unificateur. *Recherche* **7,** 919–927 (1976).
4 Rubinstein, M. & Colby, R. H. *Polymer Physics* 320 (Oxford University Press, 2003).
5 Ginzburg, V. L. Some remarks on second order phase transitions and microscopic theory of ferroelectrics. *Fiz. Tverd, Tela* **2,** 2031–2043 (1961).
6 de Gennes, P. G. Critical behaviour for vulcanization processes. *J. Phys. (France) Lett.* **38,** 355–358 (1977).
7 Daoud, M. Vulcanization and critical exponents. *J. Phys. (France) Lett.* **40,** 201–205 (1979).
8 Flory, P. J. Molecular size distribution in three dimensional polymers. I. Gelation1. *J. Am. Chem. Soc.* **63,** 3083–3090 (1941).
9 Stockmayer, W. H. Theory of molecular size distribution and gel formation in branched–chain polymers. *J. Chem. Phys.* **11,** 45–55 (1943).
10 Stockmayer, W. H. Theory of molecular size distribution and gel formation in branched polymers II. General cross linking. *J. Chem. Phys.* **12,** 125–131 (1944).
11 Stauffer, D., Coniglio, A. & Adam, M. Gelation and critical phenomena. *Adv. Polym. Sci.* **44,** 103–158 (1982).
12 de Gennes, P.-G. *Scaling Concepts in Polymer Physics* (Cornell University Press, Ithaca, NY, 1979).
13 Lusignan, C. P., Mourey, T. H., Wilson, J. C. & Colby, R. H. Viscoelasticity of randomly branched polymers in the critical percolation class. *Phys. Rev. E* **52,** 6271–6280 (1995).
14 Lusignan, C. P., Mourey, T. H., Wilson, J. C. & Colby, R. H. Viscoelasticity of randomly branched polymers in the vulcanization class. *Phys. Rev. E* **60,** 5657–5669 (1999).
15 Inoue, T., Okamoto, H. & Osaki, K. Birefringence of amorphous polymers I dynamic measurement on polystyrene. *Macromolecules* **24,** 5670–5675 (1991).
16 Schroter, K., Hutcheson, S. A., Shi, X., Mandanici, A. & McKenna, G. B. Dynamic shear modulus of glycerol: corrections due to instrument compliance. *J. Chem. Phys.* **125,** 214507 (2006).
17 Hutcheson, S. A. & McKenna, G. B. The measurement of mechanical properties of glycerol, m-toluidine, and sucrose benzoate under consideration of corrected rheometer compliance: an in-depth study and review. *J. Chem. Phys.* **129,** 074502 (2008).
18 Ferry, J. D. *Viscoelastic Properties of Polymers* 264–320 (Wiley, 1980).
19 Schosseler, F., Benoit, H., Grubisic-Gallot, Z., Strazielle, C. & Leibler, L. Gelation process by size-exclusion chromatography coupled with light scattering. *Macromolecules* **22,** 400–410 (1989).
20 Ottavi, H. Amplitude ratio of the second moments of the cluster size distribution on both sides of the percolation threshold. *J. Phys. A* **20,** 1015–1020 (1987).
21 Maeda, N. & Norisuye, T. On the unperturbed dimensions of bisphenol A polycarbonate. *Polymer* **34,** 3475–3480 (1993).
22 Yamakawa, H. *Modern Theory of Polymer Solutions* 434 (Harper & Row Publishers, 1971).
23 Weissmüller, M. & Burchard, W. Viscosity of fractions from end-linked polystyrene star macromolecules. *Acta Polym.* **48,** 571–578 (1997).
24 Inoue, T., Onogi, T. & Osaki, K. Viscoelasticity of low molecular weight polystyrene. Separation of rubbery and glassy components. *J. Polym. Sci. Polym. Phys. Ed.* **37,** 389–397 (1999).
25 Rubinstein, M., Colby, R. H. & Gillmor, J. R. *Space-Time Organization in Macromolecular Fluids* 66–74 (Springer, 1989).
26 Inoue, T. & Osaki, K. Role of polymer chain flexibility on the viscoelasticity around the glass transition zone. *Macromolecules* **29,** 1595–1599 (1996).
27 Tamura, E., Kawai, Y., Inoue, T., Matsushita, A. & Okamoto, S. Dynamic birefringence and non-linear rheology of diblock copolymer micellar solutions. *Soft Matter* **8,** 6161–6166 (2012).
28 Tamura, E., Kawai, Y., Inoue, T. & Watanabe, H. Rheo-optical study of viscoelastic relaxation modes in block copolymer micellar lattice system. *Macromolecules* **45,** 6580–6586 (2012).
29 Inoue, T., Matsumoto, A. & Nakamura, K. Dynamic viscoelasticity and birefringence of poly(ionic liquids) in the vicinity of glass transition zone. *Macromolecules* **46,** 6104–6109 (2013).
30 Maeda, A., Inoue, T. & Sato, T. Dynamic segment size of the cellulose chain in an ionic liquid. *Macromolecules* **46,** 7118–7124 (2013).

Supplementary Information accompanies the paper on Polymer Journal website (http://www.nature.com/pj)